

# Optimization strategy for element sizing in hybrid power systems

Alejandro J. del Real, Alicia Arce and Carlos Bordons

**Abstract**—This paper presents a procedure to evaluate the optimal element sizing of hybrid power systems. In order to generalize the problem, this work is based on the “energy hub” concept and formulation previously presented in the literature. The resulting optimization minimizes an objective function based on costs and efficiencies of the system elements, while taking into account the hub model, energy and power constraints and estimated operational conditions, such as energy prices, input power flow availability and output energy demand. The resulting optimal architecture also constitutes a framework for further real-time control designs.

Also, an example of a hybrid storage system is considered. In particular, the architecture of a hybrid plant incorporating a wind generator, batteries and intermediate hydrogen storage is optimized, based on real wind data and averaged residential demands. The hydrogen system integrates an electrolyzer, a fuel cell stack and hydrogen tanks. The resulting optimal cost of such hybrid power plant is compared with the equivalent hydrogen-only and battery-only systems, showing improvements in investment costs of almost 30% in the worst case.

## I. INTRODUCTION

The energy infrastructures of today are about to undergo a profound change: fossil fuel prices are raising every year while, at the same time, energy demand increases in every country. Moreover, the aim to reduce greenhouse gas emissions is moving its attention to more environmentally-friendly and sustainable energy sources. With an increased utilization of small distributed energy resources for generation of electricity and heat [1], renewable energy generation will constitute an important part of the overall energy scenario in the coming years.

One of the main problems associated with these kind of systems is the reliability and quality of the power supply. As a matter of fact, since the renewable source is intermittent, unpredictable fluctuations may appear in power output [2]. Also, electrical generation from renewable sources is not subject to demand, which creates imbalance in the system. One way to overcome this problem is by including intermediate storage, such as batteries, water pumping, super-capacitors, compressed air, fly wheels, superconducting magnetic energy storages, etc [3]. Among the most promising storage technologies are those based on hydrogen production and utilization, which is expected to be used for very different applications [4], [5] as they constitute some interesting

advantages in terms of cost, autonomy, power range and environmental effects [6].

However, hybrid energy storage systems increase the complexity of the overall power plant, the control design having an important effect on system performance. Thus, there are a number of controllers available in the literature, such as those based on heuristic rules and trial-and-error techniques [7], [8], [9], [10]. Fuzzy logic approaches [11], [12] are equivalent to those based on heuristic rules in the sense that they rely on system knowledge to obtain the ‘best’ intuitive power management. Nonetheless, other approaches based on on-line optimization can be found, resulting in a more re-usable and rigorous design process, so that the final algorithm achieves a guaranteed optimum level [13]. Along these lines, an on-line optimization to minimize the hydrogen consumption for residential hybrid power plants was presented in [14] and [15]. As for renewable sources, the intermittency of the available power also has a great impact on system performance. Although not being suitable for real-time control as the designs cited, there are some control algorithms based on prior knowledge of future conditions (such as wind speed data) which are useful as a basis of comparison for the evaluation of real-time control strategy quality [16].

As well as the control design, it is very important that component sizing be taken into account in order to reduce installation investment costs and to achieve good overall performance. However, very few papers have addressed this issue. To this end, [17] discusses the best coupling methods for conventional storage batteries with hydrogen energy storage which includes an electrolyzer, hydrogen storage tank, and a fuel cell. The resulting study shows that if multiple energy storage devices with complementary performance characteristics are used together, the resulting hybrid system can dramatically reduce the cost of energy storage over single storage systems. Also, [18] proposes a very general mathematical formulation of these hybrid power plants, the so-called “energy hubs”, which is utilized to determine the optimal coupling of energy infrastructures.

This paper, following the concept and mathematical formulation of the energy hubs presented in [18] and other related papers by the same authors such as [16], [19], [20], [21], proposes a novel optimization, which is not aimed to establishing the optimal hub layout as done in [18] but at determining the optimal hub size for a determined layout.

In the following section, energy hub concept and mathematical formulation are briefly outlined, as there is an extensive literature by the corresponding authors describing them. Section III proposes an innovative general cost

This work was supported by MEC-Spain (contract DPI2008-04568) and the European Commission (Hycon FPG-511368)

The authors are with Escuela Superior de Ingenieros, Departamento de Ingeniería de Sistemas y Automática, University of Seville, 41092 Camino de los Descubrimientos s/n, Seville, Spain. e-mail: {adelreal, aarce}@cartuja.us.es, bordons@esi.us.es

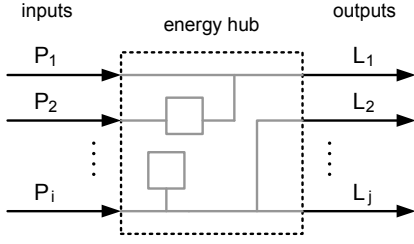


Fig. 1. General energy hub diagram

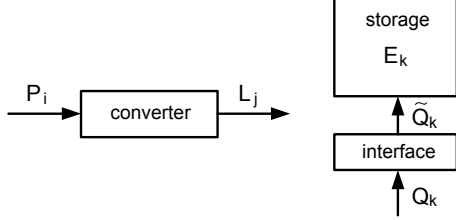


Fig. 2. Energy hub basic elements: converter (left) and storage (right)

function to minimize component sizing based on costs and efficiencies. Section IV applies the general optimization scenario to a wind generator/hydrogen/batteries power plant, also discussing the results obtained. Lastly section V is dedicated to the concluding remarks.

## II. ENERGY HUB CONCEPT AND FORMULATION

As an increased utilization of distributed generation technologies will characterize future energy systems, terms like “multiple energy carrier systems” [22] and “hybrid energy systems” [23] have become the norm when referring to systems including various forms of energy. In this way, as noted in [21], there are a number of approaches to formulate these kind of systems, such as “energy–services supply systems” [24], “basic units” [25], “microgrids” [26] and the so-called “hybrid energy hubs” [27].

The latter formulation is adopted herein, which is extensively described in the PhD thesis [21] and related publications. According to this formulation, energy hubs are defined as interfaces among energy producers, consumers, and the transportation infrastructure (see fig. 1, where  $P_i$  are power inputs and  $L_j$  power outputs), and contain three basic elements: direct connections, converters and storage (see fig. 2, with  $Q_k$  being the power exchange,  $\tilde{Q}_k$  the internal power and  $E_k$  the stored energy).

Converters link inputs and outputs through *coupling factors*  $c_{i,j}$ , which can be considered to be the converter’s steady–state energy efficiency, expressed as:

$$L_j = c_{i,j} P_i \quad (1)$$

Considering all the energy hub inputs  $\mathbf{P}$  and outputs  $\mathbf{L}$ , the following *converter coupling matrix*  $\mathbf{C}$  results:

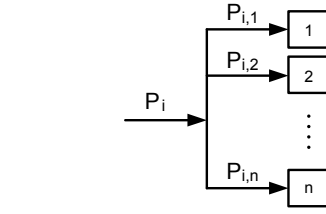


Fig. 3. Input power  $P_i$  dispatch

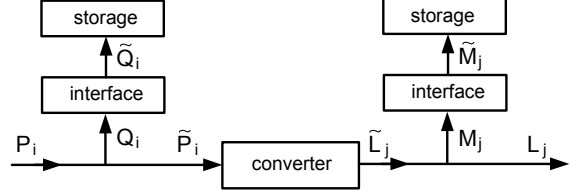


Fig. 4. Converter with storage at the input and the output sides

$$\underbrace{\begin{bmatrix} L_1 \\ \vdots \\ L_i \\ \vdots \\ L_j \end{bmatrix}}_{\mathbf{L}} = \underbrace{\begin{bmatrix} c_{1,1} & \dots & c_{i,1} \\ \vdots & \ddots & \vdots \\ c_{1,j} & \dots & c_{i,j} \end{bmatrix}}_{\mathbf{C}} \underbrace{\begin{bmatrix} P_1 \\ \vdots \\ P_j \end{bmatrix}}_{\mathbf{P}} \quad (2)$$

As the input flow  $P_i$  can be distributed among various converter devices (see fig. 3), *dispatch factors*  $v_{i,n}$  specify how much of the input power  $P_i$  flows into the converter  $n$ :

$$P_{i,n} = v_{i,n} P_i \quad (3)$$

Conservation of power also introduces the constraints

$$0 \leq v_{i,n} \leq 1 \quad \forall i, \forall n \quad (4a)$$

$$\sum_n v_{i,n} = 1 \quad \forall i \quad (4b)$$

With respect to storage, power exchange  $Q_k$  and stored energy  $E_k$  are linked through the equation:

$$\tilde{Q}_k = e_k Q_k = dE_k/dt \approx \Delta E_k / \Delta t \triangleq \dot{E}_k \quad (5)$$

$e_k$  being the efficiency of the charge/discharge storage interfaces, expressed as

$$e_k = \begin{cases} e_k^+ & \text{if } Q_k \geq 0 \quad (\text{charging/standby}) \\ 1/e_k^- & \text{else} \quad (\text{discharging}) \end{cases} \quad (6)$$

When storage elements exist, power conservation leads to the following, depending on which side of the converter the storage is located (see fig. 4):

$$\tilde{P}_i = P_i - Q_i \quad (7a)$$

$$\tilde{L}_j = L_j + M_j \quad (7b)$$

Adding the storage to the hub equation (2) leads to:

$$[\mathbf{L} + \mathbf{M}] = \mathbf{C} [\mathbf{P} - \mathbf{Q}] \quad (8)$$

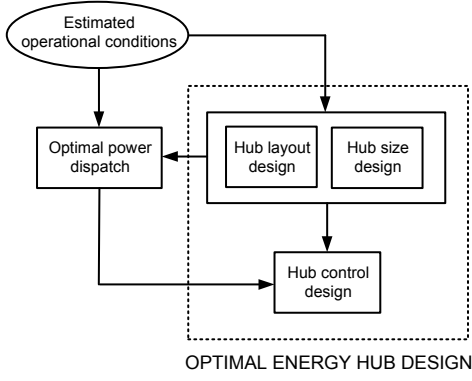


Fig. 5. Optimal energy hub design steps

Assuming a constant *converter coupling matrix*  $\mathbf{C}$  and applying superposition, the equivalent storage flows are:

$$\mathbf{M}^{eq} = \mathbf{C} \mathbf{Q} + \mathbf{M} \quad (9)$$

Rewriting (8) in a more condensed form,

$$\mathbf{L} = \mathbf{C} \mathbf{P} - \mathbf{M}^{eq} \quad (10)$$

Defining the *storage coupling matrix*  $\mathbf{S}$  to describe how changes of the storage energy derivatives affect the hub output flows, the equivalent storage power flows  $\mathbf{M}^{eq}$  can be stated as

$$\underbrace{\begin{bmatrix} M_1^{eq} \\ \vdots \\ M_k^{eq} \end{bmatrix}}_{\mathbf{M}^{eq}} = \underbrace{\begin{bmatrix} s_{1,1} & \dots & s_{1,k} \\ \vdots & \ddots & \vdots \\ s_{1,k} & \dots & s_{k,k} \end{bmatrix}}_{\mathbf{S}} \underbrace{\begin{bmatrix} \dot{E}_1 \\ \vdots \\ \dot{E}_k \end{bmatrix}}_{\mathbf{P}} \quad (11)$$

Summarizing all the previous equations, the complete hub energy model would be:

$$\mathbf{L} = \mathbf{C} \mathbf{P} - \mathbf{S} \dot{\mathbf{E}} \quad (12)$$

### III. OPTIMAL HUB SIZE

Optimal hub design can be divided into two different steps: optimal hub architecture design and hub control design (see fig. 5). Most of the papers in the literature, as mentioned in section I, are dedicated solely to the controller design, not addressing architecture design. Accordingly, different types of controllers are proposed: heuristic rules, fuzzy logic, on-line optimization, etc. The better the controller design, the better the performance of a given system. However, hub architecture and control designs are not independent from one another. As a matter of fact, the performance of the overall system not only depends on the quality of the controller but also on the hub architecture.

Optimal hub sizing for any given hub layout entails optimization of converter and storage element sizes. To that end, cost and efficiencies associated with each component, as well as the estimated working conditions of the hub (such as energy prices, input energy flows availability, output power

demand, etc.) have to be taken into account. The overall optimal architectural design results in an iterative process, evaluating the optimal cost of each hub layout in order to select the one that minimizes the investment cost while assuring a determined performance level based on the agents affecting the system.

Given the optimal hub architecture, and supposing knowledge of the system operational conditions, a suitable optimization problem minimizing a determined objective function would then represent the basis of comparison for the evaluation of real-time control strategy quality. This type of optimization problem is referred to as “optimal power dispatch” [16].

The problem presented by optimal hub sizing, which is the objective of this work, can be basically expressed with three relations: an objective function which accounts for the minimization of the system investment cost; physical laws representing the hub; and technical limitations. By making the optimization horizon as large as possible to cover the highest number of possible operational conditions and situations, the optimization is stated as a multi-period nonlinear constrained problem including an objective function, equality and inequality constraints.

The energy hub is described by the equality constraints presented in section II. Extending that formulation to consider multiple time periods, the model would be:

$$\mathbf{L}^{(t)} = \mathbf{C}^{(t)} \mathbf{P}^{(t)} - \mathbf{S}^{(t)} \dot{\mathbf{E}}^{(t)} \quad \forall t \quad (13)$$

where

$$\dot{E}_k^{(t)} = e_k^{(t)} Q_k^{(t)} - e_k^{(t-1)} Q_k^{(t-1)} \quad (14)$$

also taking into account the dispatch factor properties given by (4).

Inequality constraints correspond to the technical limitations of the converter and storage elements. Equation (15a) expresses power limits of the converters. Equations (15b) and (15c) correspond to change in storage energy limits, which are a result of the technical characteristics of the storage interfaces, while (15d) considers the energy capacity limits of the storage elements. The last inequality (15e) is also included so that stored energy at the end of the optimization period  $N_t$  is equal to or greater than the initial amount, in order to ensure sustainable storage utilization.

$$\underline{P}_{i,n} \leq v_{i,n}^{(t)} P_i^{(t)} \leq \bar{P}_{i,n} \quad \forall t, \forall i, \forall n \quad (15a)$$

$$\underline{Q}_i \leq Q_i^{(t)} \leq \bar{Q}_i \quad \forall t, \forall i \quad (15b)$$

$$\underline{M}_j \leq M_j^{(t)} \leq \bar{M}_j \quad \forall t, \forall j \quad (15c)$$

$$\underline{E}_k \leq E_k^{(t)} \leq \bar{E}_k \quad \forall t, \forall k \quad (15d)$$

$$E_k^{(0)} \leq E_k^{(N_t)} \quad \forall k \quad (15e)$$

The objective function  $\mathcal{F}$  depends on the converter and storage element limits, which are related to its size. Note that, as the charging storage interface may be different to the discharging interface,  $\bar{Q}_i$  and  $\bar{M}_j$  correspond to the charging limits, while  $\underline{Q}_i$  and  $\underline{M}_j$  are related to the discharging

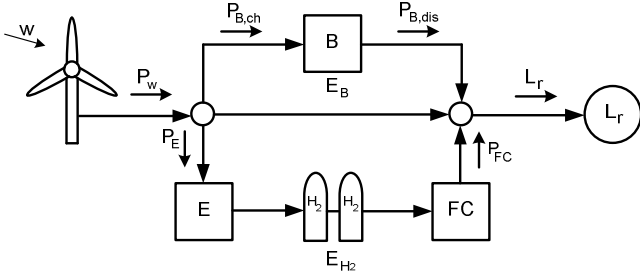


Fig. 6. Hybrid energy storage system

limits. The solution of the optimization problem provides the optimal values for the limits of the constrains (15). This way, the total objective can be expressed as:

$$\mathcal{F} = \mathcal{F}(\bar{P}_i, \bar{E}_k, \bar{Q}_i, \bar{M}_j, \underline{Q}_i, \underline{M}_j) \quad (16)$$

Considering a quadratic function, the objective remains:

$$\begin{aligned} \mathcal{F} = & \sum_i c_{\bar{P}_i} \bar{P}_i^2 + \sum_k c_{\bar{E}_k} \bar{E}_k^2 + \sum_i (c_{\bar{Q}_i} \bar{Q}_i^2 + c_{\underline{Q}_i} \underline{Q}_i^2) \\ & + \sum_j (c_{\bar{M}_j} \bar{M}_j^2 + c_{\underline{M}_j} \underline{M}_j^2) \end{aligned} \quad (17)$$

$c_{\bar{P}_i}$  being the cost per W installed of the converter  $i$ ,  $c_{\bar{E}_k}$  the cost per J installed of the storage element  $k$ , and  $c_{\bar{Q}_i}$ ,  $c_{\underline{Q}_i}$ ,  $c_{\bar{M}_j}$ ,  $c_{\underline{M}_j}$  the cost per W installed of the charging/discharging interfaces  $i$  and  $j$ .

The hub size optimization problem can finally be stated as:

$$\begin{aligned} & \text{Minimize} && \text{objective function (17)} \\ & \text{subject to} && \text{energy hub model (4),(13),(14)} \\ & && \text{energy and power constraints (15)} \end{aligned}$$

When the objective function is convex and the constraints are expressed as linear equations, the global optimum can be found utilizing numerical methods, as the solution space is convex.

#### IV. APPLICATION

Considering the system shown in fig. 6, the primary energy source is a wind generator, which is connected to a residential load ( $L_r$ ). The electricity produced via wind ( $w$ ) can be delivered to the load and/or be diverted to an electrolyzer ( $E$ ) and batteries ( $B$ ). The energy consumed by the electrolyzer ( $Q_E$ ) is used to produce hydrogen, which is stored in the tanks placed in the hydrogen line ( $E_{H_2}$ ). The fuel cell stack ( $FC$ ), fed by those tanks, can produce electricity ( $Q_{FC}$ ). Similarly, the batteries can be charged ( $Q_{B,ch}$ ), storing the energy ( $E_B$ ), and discharged ( $Q_{B,dis}$ ), thus complementing the total power supplied to the load.

Deriving this specific case from the general problem, and assuming a certain set of operational conditions, the optimal hub sizing for the proposed system is calculated. To that end, the optimization problem is formulated as in the previous section III

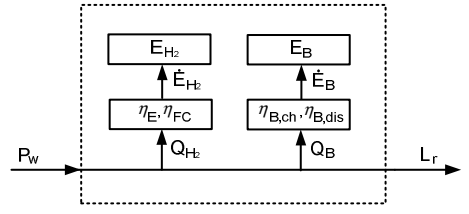


Fig. 7. Corresponding energy hub of a hybrid energy storage system

TABLE I  
HYBRID ENERGY STORAGE SYSTEM EFFICIENCIES

Hub element	Efficiency
Electrolyzer	$\eta_E = 0.74$
Fuel cell	$\eta_{FC} = 0.47$
Battery charging	$\eta_{B,ch} = 0.7$
Battery discharging	$\eta_{B,dis} = 0.9$

#### A. Energy hub model

Model equations are based on the notation presented in section II. This way, the specific energy hub is illustrated in fig. 7. Input, output and storage energy derivative vectors for multiple time periods, can be defined as

$$\mathbf{P}^{(t)} = \begin{bmatrix} P_w^{(t)} \end{bmatrix} \quad (18a)$$

$$\mathbf{L}^{(t)} = \begin{bmatrix} L_r^{(t)} \end{bmatrix} \quad (18b)$$

$$\dot{\mathbf{E}}^{(t)} = \begin{bmatrix} \dot{E}_{H_2}^{(t)} & \dot{E}_B^{(t)} \end{bmatrix}^T \quad (18c)$$

Also, following the aforementioned notation, *converter coupling matrix*  $\mathbf{C}^{(t)}$  and *storage coupling matrix*  $\mathbf{S}^{(t)}$  are stated as:

$$\mathbf{C}^{(t)} = \begin{bmatrix} 1 \end{bmatrix} \quad (19)$$

$$\mathbf{S}^{(t)} = \begin{bmatrix} 1/e_{H_2}^{(t)} & 1/e_B^{(t)} \end{bmatrix} \quad (20)$$

where  $e_{H_2}^{(t)}$  and  $e_B^{(t)}$  are the storage interface efficiencies (see table I), the electrolyzer being the ‘charging’ interface and the fuel cell the ‘discharging’ interface for the hydrogen line. Also, notice that different battery charging and discharging efficiencies are considered, resulting in the following relations:

$$e_{H_2}^{(t)} = \begin{cases} \eta_E & \text{if } Q_{H_2}^{(t)} \geq 0 \text{ (electrolyzer)} \\ 1/\eta_{FC} & \text{else (fuel cell)} \end{cases} \quad (21a)$$

$$e_B^{(t)} = \begin{cases} \eta_{B,ch} & \text{if } Q_B^{(t)} \geq 0 \text{ (battery charging)} \\ 1/\eta_{B,dis} & \text{else (battery discharging)} \end{cases} \quad (21b)$$

with the power exchanges  $Q_{H_2}^{(t)}$ ,  $Q_B^{(t)}$  and storage energy derivatives  $\dot{E}_{H_2}^{(t)}$ ,  $\dot{E}_B^{(t)}$  expressed as:

TABLE II

HYBRID ENERGY STORAGE ELEMENT COSTS

Hub element	Cost
Wind power	$c_{\bar{P}_w} = \$2/W$
Electrolyzer	$c_{\bar{Q}_E} = \$1.9/W$
Fuel cell	$c_{\bar{Q}_{FC}} = \$2.5/W$
Hydrogen tank	$c_{\bar{E}_{H_2}} = \$0.03/Wh$
Battery	$c_{\bar{E}_B} = \$0.2/Wh$

$$\dot{E}_{H_2}^{(t)} = e_{H_2}^{(t)} Q_{H_2}^{(t)} - e_{H_2}^{(t-1)} Q_{H_2}^{(t-1)} \quad (22a)$$

$$\dot{E}_B^{(t)} = e_B^{(t)} Q_B^{(t)} - e_B^{(t-1)} Q_B^{(t-1)} \quad (22b)$$

### B. Energy and power constraints

Technical limitations are modeled as they were in (15). Input power limits, storage interfaces power exchange capacities and stored energy limitations are evaluated next.

With respect to the input, wind power  $P_w^{(t)}$  depends on the available wind power, as well as on the size of the wind generator. Defining  $\hat{P}_w^{(t)}$  as the normalized power produced by a 1W wind generator given a certain wind speed at time  $t$ , power input limits would be:

$$\left[ 0 \right] \leq \left[ P_w^{(t)} \right] \leq \left[ \hat{P}_w^{(t)} \bar{P}_w \right] \quad (23)$$

with  $\bar{P}_w$  being the size of the wind generator of the proposed hybrid storage plant.

Power storage exchange is also limited by the maximum power that can be provided by the storage interfaces:

$$\left[ \begin{array}{c} -\bar{Q}_{FC} \\ -\bar{Q}_{B,dis} \end{array} \right] \leq \left[ \begin{array}{c} Q_{H_2}^{(t)} \\ Q_B^{(t)} \end{array} \right] \leq \left[ \begin{array}{c} \bar{Q}_E \\ \bar{Q}_{B,ch} \end{array} \right] \quad (24)$$

whereas for the hydrogen line,  $\bar{Q}_E$  and  $\bar{Q}_{FC}$  represent the maximum capacities of electrolyzer and fuel cell respectively. Concerning the batteries,  $\bar{Q}_{B,ch}$  and  $\bar{Q}_{B,dis}$  are the limit charging/discharging rates. Notice that these rates are usually a function of total battery size  $\bar{E}$ , assuming here that  $\bar{Q}_{B,ch} = 0.2\bar{E}$  and  $\bar{Q}_{B,dis} = 2\bar{E}$ .

Maximum stored energy depends on the size of the hydrogen tanks  $\bar{E}_{H_2}$  and the batteries  $\bar{E}_B$ . Due to technical constraints, the batteries should never be totally drained nor fully charged; they should always be in a partially charged state. Taking these considerations into account and assuming a safe charge level, the constraint can be expressed as:

$$\left[ \begin{array}{c} 0 \\ 0.2\bar{E}_B \end{array} \right] \leq \left[ \begin{array}{c} E_{H_2}^{(t)} \\ E_B^{(t)} \end{array} \right] \leq \left[ \begin{array}{c} \bar{E}_{H_2} \\ 0.9\bar{E}_B \end{array} \right] \quad (25)$$

Finally, a constraint to verify sustainable energy storage is also introduced, so that

$$\left[ \begin{array}{c} E_{H_2}^{(0)} \\ E_B^{(0)} \end{array} \right] \leq \left[ \begin{array}{c} E_{H_2}^{(N_t)} \\ E_B^{(N_t)} \end{array} \right] \quad (26)$$

### C. Objective function

Moving from the general (17) to the specific, the objective function, whose cost terms are shown in table II [17], would be:

$$\mathcal{F} = c_{\bar{P}_w} \bar{P}_w^2 + c_{\bar{E}_{H_2}} \bar{E}_{H_2}^2 + c_{\bar{E}_B} \bar{E}_B^2 + c_{\bar{Q}_{FC}} \bar{Q}_{FC}^2 + c_{\bar{Q}_E} \bar{Q}_E^2 \quad (27)$$

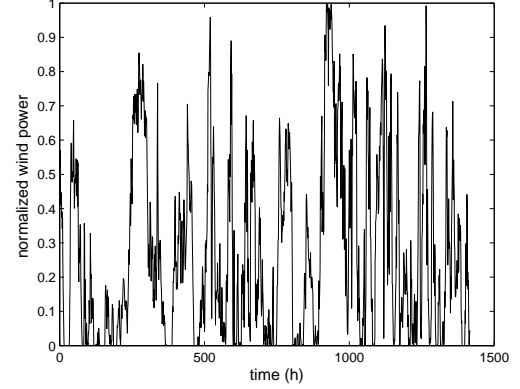


Fig. 8. Normalized wind power data set (recorded over a two-month period)

### D. Operational conditions

As the optimal hub architecture design is based on estimated operational conditions, the more precise the utilized data are, the more accurate are the architectural results. As for the power input, a two-month wind power normalized data set  $\hat{P}_w^{(t)}$  was considered (see fig 8). Concerning the load  $L_r$ , the data used is shown in fig. 9, which represents the average daily load for the residential sector in Spain [28]. The sampling time for all the data sets is 1h.

### E. Optimization results

The optimization was done for three hub layouts: hybrid, hydrogen-only and battery-only storage, and was implemented in Matlab using the solver "CPLEX", resulting in a

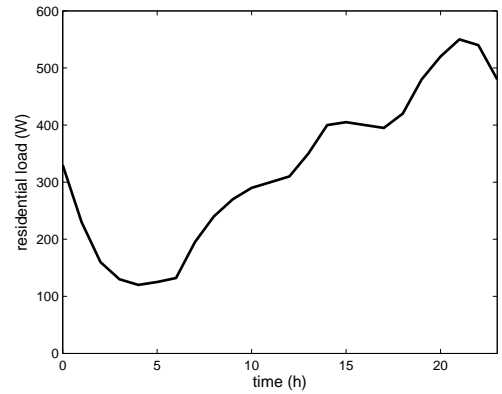


Fig. 9. Residential sector average daily loads

TABLE III  
HYBRID ENERGY STORAGE SYSTEM COSTS

Equipment	Hybrid	Hydrogen-only	Battery-only
	cost (size)	cost (size)	cost (size)
Wind generator	\$7600 (3800 W)	\$8600 (4300 W)	\$12500 (6250 W)
Electrolyzer	\$656 (345 W)	\$665 (350 W)	—
Fuel cell	\$450 (180 W)	\$1375 (550 W)	—
H <sub>2</sub> tank	\$1642 (54.730 kWh)	\$3681 (122.695 kWh)	—
Batteries	\$2268 (11.34 kWh)	—	\$3651 (18.255 kWh)
Total cost	\$12616	\$14321	\$16151
Increment	Baseline	11.91%	28.02%

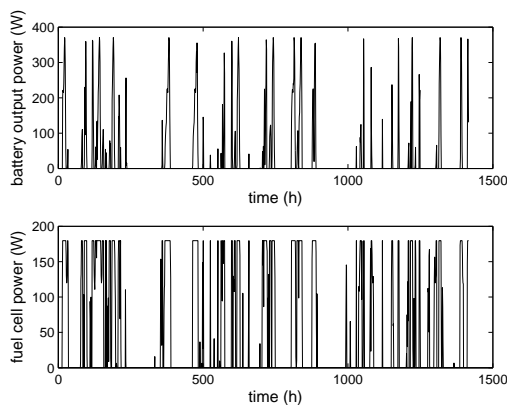


Fig. 10. Optimal utilisation of battery (upper graph) and fuel cell (lower graph) for a hybrid storage power system

Mixed Integer Quadratic Programming (MIQP). Confirming the studies presented in [17], hybrid storage proved to be significantly cheaper than other possible storage systems. In particular, hydrogen-only storage cost is 11.91% higher than the hybrid plant, the battery-only choice being 28.02% more expensive than such hybrid system (see table III for detailed information).

As can be seen in fig. 10, hybrid storage layout combines the best characteristics of both energy storage devices. In particular, the fuel cell is used as a base power supplier, while batteries are utilized to deliver the power peaks. In a hydrogen-only choice, the fuel cell size has to be increased in order to create the power peaks, which results in a cost increase due to the high cost of the equipment. On the other hand, battery-only storage requires a large total energy capacity, which is costly too.

## V. CONCLUDING REMARKS

In this paper, an optimization strategy for sizing hybrid power systems is presented. The mathematical formulation is based on the “energy hub” concept described in previous literature. The optimization procedure was applied to a hybrid

power plant incorporating a wind generator, conventional batteries and a hydrogen storage system comprised of a fuel cell, an electrolyzer and hydrogen tanks. The optimal architecture resulted in a 30% improvement among the possible system layouts in terms of cost effectiveness.

## VI. ACKNOWLEDGMENTS

The authors gratefully acknowledge the contribution of Carlos Pardo, who is working on his master thesis in related issues.

## REFERENCES

- [1] A. M. Borbely and J. F. Kreider, Eds., *Distributed Generation: The Power Paradigm for the New Millennium*. Boca Raton: CRC Press, 2001.
- [2] D. Anderson and M. Leach, “Harvesting and redistributing renewable energy: On the role of gas and electricity grids to overcome intermittency through the generation and storage of hydrogen,” *Energy policy*, vol. 32, pp. 1603–1614, 2004.
- [3] R. Dell and D. Rand, “Energy storage—a key technology for global energy sustain,” *Journal of Power Sources*, vol. 100, pp. 2–17, 2001.
- [4] E. Leal and J. Silveira, “Study of fuel cell co-generation systems applied to a dairy industry,” *J. Power Sources*, vol. 106, no. 1, pp. 102–108, 2002.
- [5] A. Lokurlu, T. Grube, B. Hohlein, and D. Stolten, “Fuel cells for mobile and stationary applications—cost analysis for combined heat and power stations on the basis of fuel cells,” *Int. J. Hydrogen Energy*, vol. 28, no. 7, pp. 703–711, 2003.
- [6] J. Kaldellis and D. Zafirakis, “Optimum energy storage techniques for the improvement of renewable energy sources-based electricity generation economic efficiency,” *Energy*, 2007.
- [7] O. Onar, M. Uzunoglu, and M. Alam, “Dynamic modeling, design and simulation of a wind/fuel cell/ultra-capacitor-based hybrid power generation system,” *J. Power Sources*, vol. 161, pp. 707–722, 2006.
- [8] S. Kélouwani, K. Agbossou, and R. Chahine, “Model for energy conversion in renewable energy system with hydrogen storage,” *J. Power Sources*, vol. 140, pp. 392–399, 2005.
- [9] J. Vanhanen, P. Kauranen, P. Lund, and L. Manninen, “Simulation of solar hydrogen energy systems,” *Solar Energy*, vol. 53, no. 3, pp. 267–278, 1994.
- [10] A. Arce, A. del Real, and C. Bordons, “Power management heuristic control for a hybrid fuel cell vehicle (in spanish),” in *XXVIII Jornadas de Automática*, 2007.
- [11] K. Jeong, W. Lee, and C. Kim, “Energy management strategies of a fuel cell/battery hybrid system using fuzzy logics,” *J. Power Sources*, vol. 145, pp. 319–326, 2005.
- [12] A. Bilodeau and K. Agbossou, “Control analysis of renewable energy system with hydrogen storage for residential applications,” *J. Power Sources*, vol. 162, pp. 757–764, 2006.
- [13] A. Schell, H. Peing, D. Tran, E. Stamos, C. Lin, and M. Kim, “Modelling and control strategy development for fuel cell electric vehicles,” *Annual Reviews in Control*, vol. 29, pp. 159–168, 2005.
- [14] I. Valero, S. Bacha, and E. Rulliere, “Comparison of energy management controls for fuel cell applications,” *J. Power Sources*, vol. 156, pp. 50–56, 2006.
- [15] A. del Real, A. Arce, and C. Bordons, “Hybrid model predictive control of a two-generator power plant integrating photovoltaic panels and a fuel cell,” in *Proc. 2007 Conference on Decision and Control*, New Orleans, LA, Dec. 2007.
- [16] M. Geidl and G. Andersson, “Optimal power dispatch in systems with multiple energy carriers,” in *Proc. of 15th Power Systems Computation Conference*, Liege, Belgium, 2005.
- [17] S. Vosen and J. Keller, “Hybrid energy storage systems for stand-alone electric power systems: optimization of system performance and cost through control strategies,” *Int. J. Hydrogen Energy*, vol. 24, pp. 1139–1156, 1999.
- [18] M. Geidl and G. Andersson, “Optimal coupling of energy infrastructures,” in *Proc. of IEEE PES PowerTech*, Lausanne, Switzerland, 2007.
- [19] M. Geidl, G. Koeppel, P. Favre-Perrod, B. Klöckl, G. Andersson, and K. Fröhlich, “Energy hubs for the future,” *IEEE Power and Energy Magazine*, vol. 5, no. 1, pp. 24–30, 2007.

- [20] M. Geidl and G. Andersson, "Optimal power flow of multiple energy carriers," *IEEE Transactions on Power Systems*, vol. 22, no. 1, pp. 145–155, 2007.
- [21] M. Geidl, "Integrated Modeling and Optimization of Multi-Carrier Energy Systems," Ph.D. dissertation, ETH, Zurich, 2007.
- [22] B. Bakken, A. Haugstad, K. S. Hornnes, and S. Vist, "Simulation and optimization of systems with multiple energy carriers," in *Proc. of Scandinavian Conference on Simulation and Modeling*, Linköping, Sweden, 1999.
- [23] J. F. Manwell, "Hybrid energy systems," *Encyclopedia of Energy*, vol. 3, pp. 215–229, 2004.
- [24] H. M. Groscurth, T. Bruckner, and R. Kümmel, "Modeling of energy-services supply systems," *Energy*, vol. 20, no. 9, pp. 941–958, 1995.
- [25] I. Bouwmans and K. Hemmes, "Optimising energy systems–hydrogen and distributed generation," in *Proc. of 2nd International Symposium on Distributed Generation*, Stockholm, Sweden, 2002.
- [26] R. H. Lasseter, "Microgrids," in *Proc. of IEEE PES Winter Meeting*, New York, USA, 2002.
- [27] R. Frick and P. Favre-Perrod, "Proposal for a multifunctional energy bus and its interlink with generation and consumption," Master's thesis, ETH, High Voltage Laboratory, Zurich, 2004.
- [28] "Proyecto INDEL: Atlas de la Demanda Eléctrica Española," Red Eléctrica de España, Tech. Rep., 1997.